Available online at www.sciencedirect.com
SCIENCE DIRECT®
Polymer 45 (2004) 3441–3455
polymer
www.elsevier.com/locate/polymer

Lamellar morphology of random metallocene propylene copolymers studied by atomic force microscopy

Ian L. Hosier[a], Rufina G. Alamo[a,*], J.S. Lin[b]

[a]*Department of Chemical Engineering, FAMU-FSU College of Engineering, 2525 Pottsdamer Street, Tallahassee, FL 32310, USA*
[b]*Oak Ridge National Laboratory, Oak Ridge, TN 37831, USA*

Received 23 July 2003; received in revised form 24 February 2004; accepted 26 February 2004

Abstract

Four sets of propylene based random copolymers with co-units of ethylene, 1-butene, 1-hexene and 1-octene, and a total defect content up to ~9 mol% (including co-unit and other defects), were studied after rapid and isothermal crystallization. Etched film surfaces and ultramicrotomed plaques were imaged so as to enhance contrast and minimize catalyst and co-catalyst residues. While increasing concentration of structural irregularities breaks down spherulitic habits, the formation of the gamma polymorph has a profound effect on the lamellar morphology. Lamellae grown in the radial axis of the spherulite and branches hereon are replaced in γ-rich copolymers with a dense array of short lamellae transverse or tilted to the main structural growth axis. This is the expected orientation for γ *i*PP branching from α seeds. Spherulites are formed in copolymers with non-crystallizable units (1-hexene and 1-octene) up to ~3 mol% total defect content and were observed up to ~6 mol% in those with partially crystallizable comonomers (ethylene and 1-butene). However, lamellae were observed in all the copolymers analyzed, even in the most defective ones, highlighting the important role of the gamma polymorph in propagating lamellar crystallites in poly(propylenes) with a high concentration of defects. Long periods measured from AFM and SAXS are comparatively analyzed.

Keywords: Propylene Copolymers; Morphology; Atomic force microscopy

1. Introduction

Understanding the effects of chain microstructure on the morphology and crystallization behavior of poly(propylene) and its copolymers is key to applying these materials to an ever diversifying range of applications. A major advance in expanding the properties of poly(propylenes) is the advent of metallocene catalysts, which allow incorporation of large contents of comonomer, copolymerization of cyclic and other comonomer types that are not easily incorporated with classical Ziegler Natta (ZN) catalysts and excellent control of stereoregularity. These catalysts lead to a new class of random polyolefins, which are inaccessible through conventional heterogeneous ZN catalysts [1,2].

The series of propylene copolymers studied in this work were synthesized with a metallocene catalyst that yields random comonomer distribution, uniform intermolecular distribution of the comonomer content and narrow molecular weight distribution. Hence, these copolymers allow the study of their crystalline structure as a function of increasing comonomer content and, for different types of comonomer at the same comonomer concentration, while other molecular variables such as molar mass and comonomer distribution remain constant. In previous works, the partitioning of the comonomer unit [3] and the conditions for the formation of the alpha and gamma polymorphs [4] were studied in detail in the same copolymers. The effect of the comonomer in enhancing the fractional content of the gamma polymorph was found to be the same as the role of defects in the homo poly(propylene) chain. Thus, independent of the chemical nature of the co-unit, as the comonomer and/or crystallization temperature increase, the fractional content of the gamma polymorph increases at the expense of the alpha phase. However, differences in the partitioning of the ethylene, l-butene, l-hexene and l-octene units between the crystalline and non-crystalline regions leads to contents of the gamma phase that differ among the copolymers [4].

* Corresponding author. Tel.: +1-850-410-6376.
E-mail address: alamo@eng.fsu.edu (R.G. Alamo).

0032-3861/$ - see front matter © 2004 Elsevier Ltd. All rights reserved.
doi:10.1016/j.polymer.2004.02.071

As the gamma phase is favored in *i*PPs with short crystallizable sequences, higher gamma contents were found in propylene l-hexenes (PHs) and propylene l-octenes (POs) in which the co-units are rejected from the crystal lattice. In the present work, we extend the on-going structural studies of these copolymers to analyze the lamellar morphologies that develop as a function of increasing crystallization temperature in the same copolymers. The crystallization temperatures are chosen in a range such that each copolymer developed up to 100% of the gamma polymorph. In this manner, the associated lamellar structures corresponding to the pure polymorphs and their mixtures could be identified. Simultaneously, the role of comonomer content on the morphology was also studied. The overall spherulitic morphology was characterized by optical microscopy complemented by scanning electron microscopy (SEM), and the details of the lamellar morphology were quantified by atomic force microscopy (AFM). The simplicity of sample preparation is the major advantage of AFM over transmission electron microscopy (TEM) for a detailed study of lamellar structure. Coupled with permanganic etching [5], the AFM is now recognized as a powerful tool for the characterization of polymeric materials [6–11]. In the present study, permanganic etching not only enhanced contrast, but also helped to minimize catalyst and co-catalyst residues on the surface of these copolymers that interfered with AFM imaging. The AFM data was used to characterize lamellar long periods, which were then compared to those obtained from classical SAXS methods.

2. Experimental

2.1. Materials

The propylene copolymers and homopolymer studied herein were synthesized with the same metallocene-type catalyst to ensure a very similar molecular mass and similar concentration of stereo and regio-types of defects. Characterization details are listed in Table 1. The copolymer designation is the same as that used in a previous study using the same samples [4]. Listed in separate columns are molar concentrations of the comonomer, head to head misinsertions of the erythro type and concentration of stereo defects. Defects due to hydrogen abstraction (1, 3 type) were absent in these samples. The total concentration of all types of defects added to the concentration of comonomer is also listed in this table, and the analysis of experimental data throughout the text is referred to this value. PE and PH copolymers are available in a range of comonomer contents between 0.3 and 7.5 mol%. These two sets allow a systematic study of the effect of increasing comonomer on the crystalline morphology, while other molecular variables like molar mass and fractions of stereo and regio defects are kept constant. The effect of the type of comonomer (ethylene, 1-butene, 1-hexene or 1-octene) on the morphology will also be probed by comparing the properties of the copolymers with approximately 3.3 mol% total defects. The type and fractional content of all the defects was obtained by solution ^{13}C NMR [3,4].

2.2. Crystallization procedures and film preparation for AFM studies

The morphology was studied on films of nominal thickness 0.2 mm crystallized between clean glass cover slips. To prevent degradation during the subsequent isothermal crystallization, stacks of cover slips containing films of different copolymers were placed in glass tubes and sealed in vacuum. The samples contained in evacuated tubes were melted at 180 ± 1 °C for 20 min and then quickly transferred to a second silicone oil bath maintained at the required crystallization temperature with ±0.1 °C control. Crystallization temperatures and times were used as follows; 100 °C overnight, 110 °C 3 days, 120 °C 1 week, 125 °C 2 weeks and 130 °C, 3–4 weeks. These crystallization temperatures ensured that all but the highest defect content co-polymers at the highest crystallization temperatures crystallized to completion as inferred by the absence of a quenching peak when subsequently melted in a DSC (Perkin Elmer DSC-7). After the required crystallization time had elapsed, the tubes were quenched into a water bath held at 25 °C, samples were then removed once the contents had returned to ambient conditions. For subsequent examination, one of the cover slips was easily removed without deforming the specimen with the aid of ice water or liquid N_2.

In addition, for the study of the internal microstructure, 0.5 mm thick plaques were melt compressed within aluminum foils and crystallized at 120 °C as described above. These plaques were then microtomed at −40 °C to expose an internal surface. A Microstar MS1 cryo-ultramicrotome was used with freshly cut glass knives. The plaques displayed the same melting behavior as the films, hence, the crystallization was identical in both preparations.

For initial AFM investigations the films were mounted directly onto metal AFM stubs using double-sided adhesive tape and imaged by AFM without any additional preparation. However, most of the images showed large impurities that interfered with the resolution of the lamellae. In addition, the unetched bulk samples showed significant microtome knife damage. To improve contrast, the surfaces were subjected to permanganic etching following the technique of Olley et al. [5]. The reagent used was 1% w/v $KMnO_4$ dissolved in an acid mixture of one part distilled water, four parts phosphoric acid (85% conc.) and 10 parts sulphuric acid (96% conc.). The total etching time was 10 min and the etchant was changed halfway through the procedure. The mixture was quenched in a solution of one part H_2O_2 (30% conc.) in four parts of a 2:7 sulphuric

Table 1
Molecular characterization of metallocene homopolymer and metallocene propylene copolymers

Sample	Comonomer type	Comonomer (mol%)	Regio (mol%)	Stereo (mol%)	Total defects (mol%)	M_w (g/mol)	M_w/M_n
M170K1.70	–	0.0	0.8	0.9	1.7	169,800	1.80
PE1.8	Ethylene	0.8	0.4	0.6	1.8	233,100	1.98
PE2.8	Ethylene	1.7	0.4	0.7	2.8	221,300	1.81
PE3.3	Ethylene	2.1	0.5	0.7	3.3	210,000	1.77
PE3.4	Ethylene	2.2	0.5	0.7	3.4	214,800	1.75
PE5.8	Ethylene	4.6	0.4	0.8	5.8	251,000	2.12
PE8.2	Ethylene	7.0	0.5	0.7	8.2	185,300	1.86
PE8.7	Ethylene	7.5	0.4	0.8	8.7	188,000	1.71
PB3.4	1-Butene	1.7	0.8	0.9	3.4	216,500	1.70
PB4.8	1-Butene	3.2	0.7	0.9	4.8	~210,000	1.85
PH2.0	1-Hexene	0.3	0.7	1.0	2.0	245,000	1.83
PH2.2	1-Hexene	0.6	0.7	0.9	2.2	~230,000	
PH3.2	1-Hexene	1.6	0.7	0.9	3.2	~210,000	
PH3.5	1-Hexene	1.8	0.7	1.0	3.5	206,800	1.71
PH4.3	1-Hexene	2.7	0.7	0.9	4.3	217,000	2.53
PO2.9	1-Octene	1.3	0.7	0.9	2.9	202,300	1.76

acid:water mixture previously cooled to ~0 °C in an ice/water bath. Following etching, the samples were washed several times in distilled water, rinsed in methanol and then dried under vacuum overnight.

2.3. Techniques

Long range supermolecular morphology up to ~0.5 mm^2 was characterized by optical microscopy (OM) in ~30 μm thick films. Micrographs were obtained between crossed polarizers at room temperature using an Olympus BH-2 optical microscope fitted with an Olympus DP12 digital camera.

AFM images were obtained using the environmental Jeol 4210 scanning probe microscope operating under ambient conditions. A standard silicon calibration grid (Pacific Nanotechnology) was used to check the calibration of the AFM scanner for both width and height measurements, before quantitative work was carried out and at regular intervals throughout. Topography and phase images were simultaneously collected in non-contact AC mode at 256 × 256 standard resolution. Olympus single side coated silicon cantilevers were used with resonant frequency at ~300 KHz. According to the manufacturers specifications, these cantilevers have spring constants of ~40 N/m and the radius of the tip is <10 nm.

Cross-section profiles from the AFM images, generated by the Jeol AFM process software, were used to estimate thicknesses by combining two methods; from the topographic images, the heights of flat on lamellae were estimated following a similar method as that described by Sutton et al. [7]. It is assumed that such data include the non-crystalline layers [9] and, hence, are taken as a measure of the lamellar long period when suitably oriented crystals are chosen. Additional data of lamellar long periods were obtained from measurements of the periodicity of edge on crystals (measured from valley to valley on the profiles) from both phase and topographic images of ≤2 × 2 μm size. Data from flat on and edge on crystals agreed closely and were combined to give the final distributions. At least 80 crystallites were measured in each specimen. The data were plotted in the form of histograms using half the standard deviation as the bin width [8,9]. After AFM investigation, selected films were coated with Au/Pt and imaged in a Scanning Electron Microscope (Jeol JSM 840 SEM) operating at 15 kV.

Small angle X-ray scattering was performed at the Oak Ridge National Laboratory in Tennessee. Plaques 20 × 13 × 0.5 mm were prepared using the same procedure outlined above. Intensities were collected with Cu Kα radiation at 40 kV and 100 mA. The intensity data was corrected for sample thickness, detector sensitivity, dark current and background scattering. Average lamellar long periods were taken at the peak of the Lorentz corrected SAXS intensity.

3. Results and discussion

3.1. Structural features of the α and γ polymorphs

Before analyzing the microscopic images, the main structural details of the α and γ polymorphs and related superlamellar morphologies are reviewed in this section.

The crystallographic features and superlamellar organization of the α polymorph have been described in different reviews [12–15]. The most common monoclinic unit cell, with dimensions $a = 6.65$ Å, $b = 20.96$ Å, $c = 6.50$ Å and $\beta = 99.8°$ comprises four 3_1 helical chains. The symmetry in this cell calls for alternation in the helical handness in a way such that looking in the b direction, left and right handed bilayers are seen parallel to the ac plane [16]. The lamellar morphology of α-*i*PP displays an unusual branching unique to this polymorph. Nearly normal α branching

develops via homoepitaxial growth on the 010 plane of a 'parent' lamellae as schematically represented in Fig. 1. Tangential α branching is explained as a consequence of the deposition of one layer of helices with the same chirality as the previous layer. This 'wrong' packing is possible when isochiral helices are tilted about 80° to the helices in the 010 face, resulting in nearly orthogonal growth as shown in the figure. Work by Lotz and coworkers [16] established that transverse α branching is favored by a good interdigitation of the methyl groups and the near identity of the a and c axis of the unit cell.

Epitaxial α branching from α-*i*PP leads to the unique mesh-type cross-hatched morphology described as 'quadrites' by Khoury [14] and observed since the early 1960's [17,18]. The near transverse orientation of branched lamellae may affect the overall sign of the birefringence of spherulites and might even confer a positive character if the population of lamellae transverse to the radius of the spherulite is profuse. The development of lamellar branching in homo poly(polypropylenes) is affected by isotacticity, undercooling and degree of transformation and the impact on optical properties has been recently summarized by Lotz [19]. Positive, negative or mixed spherulites develop depending on the relative proportion of radial and transverse lamellae and on the orientation of the radial lamellae relative to the path of light. Spherulites with a negative character develop at the highest and lowest undercoolings due to a reduced frequency of branching, while most often mixed spherulites develop at intermediate undercoolings. In some favorable conditions and with prolonged crystallization time, mixed spherulites acquire positive character [20].

The orthorhombic structure of the γ phase, elucidated by Meille and Brückner [21], is unprecedented in crystalline polymers in that it comprises non-parallel chains. The lattice parameters are $a = 8.54$ Å, $b = 9.93$ Å, $c = 42.4$ Å. The γ form has been structurally associated with the α through the notion that the deposition of one layer with the wrong conformation that leads to near orthogonal branching in the α phase, appears as the element of symmetry in the γ form [12,22]. Repeated in the γ phase are successive bilayers, each layer made of right or left handed helices, each bilayer faces an adjacent one via isochiral helices, hence, consecutive bilayers tilt at 80°. One, then, expects that the 010 faces of alpha crystallites will be ideal surfaces for the epitaxial crystallization of gamma crystallites, as observed in Refs. [13,22]. In fact, the growth of γ crystallites have been almost invariably related to the presence of some α seeds. To perpetuate symmetric molecular orientation within the lattice, γ lamellae branch at an angle of 40° to the α surface and the chains in the γ phase are tilted at 40° to the lamellae normal as schematically shown in Fig. 1. As a consequence, the orientation of γ branching from radial 'parent' or transverse 'daughter' *i*PP is equivalent and will appear transverse to the radial growth, as reported by Lotz et al. [23]. Heavily tilted γ lamellae from α laths have been experimentally observed after crystallization of very thin films, usually cast from solution [18,24].

The details of crystal growth in the *pure* gamma phase seem more elusive. Pure gamma crystals have shown stacked lamellar overgrowths with triangular tips consistent with the structural α−γ growth relation [24] and in agreement with earlier speculations that alpha seeds propagate γ growth [12]. However, the mechanism that allows such a careful selection of right or left helical sequences leading to gamma growth instead of alpha branching remains unknown.

The non-equivalent directions of lamellar growth of both polymorphs, as they relate to the spherulitic linear growth, should be of relevance in the analysis of nucleation and growth of these systems. Growth proceeds via the a^* axis in the α phase, oriented in the radial axis of the spherulite, while in the γ polymorph growth is perpetuated via the c axis, tilted to the radial axis. Because in the gamma phase

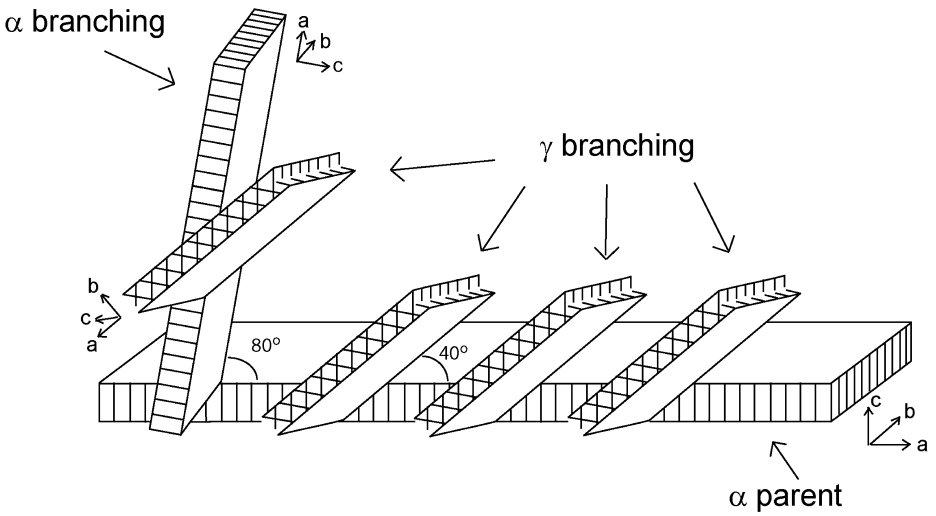

Fig. 1. Schematic model of α-*i*PP and γ-*i*PP branching from α 'parent' lamellae. The crystallographic axes are indicated. Adapted from similar schemes in Refs. [12,23].

the *c* axis is normal to the chain axis (as seen in Fig. 1), lamellar growth is taken to proceed through chain stratification [12,13]. This growth mechanism coupled with the fact that formation of the γ polymorph is favored by short isotactic sequences, led to initial speculation of the reduced importance of chain folding in propagating lamellar habits within this polymorph [25].

The complexities associated with growth of both polymorphs and their epitaxial relation, make prediction of all possible morphologies, as well as identification of each phase from microscopic images, a rather difficult task, especially when both polymorphs coexist in similar contents. The copolymers studied here develop contents of these polymorphs that change from α rich to γ rich phases (4), hence, different lamellar morphologies are expected to develop according to the characteristic growth of each phase. While α rich spherulitic morphologies, characteristic of the highest undercoolings, may develop arrays of radially oriented α and cross hatched lamellae, increasing crystallization temperature α branching may be replaced by the heavily tilted, energetically favored, γ branching. Furthermore, pure γ or γ-rich morphologies may be characterized by a diminished or absence of branching as previously stated [21], because the mechanism leading to branching in the α phase corresponds to normal growth in the γ. In addition to changes in the lamellar structure with undercooling, a degradation of the spherulitic or supermolecular morphology is also expected with the increase of comonomer in the chain, as observed in other random olefin copolymers.

3.2. Effect of increasing defect content on lamellar morphology

Focus is given to the series of propylene ethylenes (PEs) and propylene 1-hexenes (PHs) for which the greatest range in comonomer content is available. Each copolymer was isothermally crystallized at temperatures (T_c) of 100, 110, 120, 125 and 130 °C for increasing times in order to change in as large range as possible the relative concentrations of the alpha and gamma polymorphs [4]. The fraction of γ crystals, obtained in a previous work, is shown in Fig. 2 for the same PE series to facilitate the discussion of the correlation of α and γ branching with lamellar structure and the sign of the birefringence.

High nucleation density and fast growth rates in any of the copolymers crystallized at 100 °C led to heavily impinged spherulites, too small to obtain any clear micrograph. With increasing crystallization temperature the structures are better resolved. Representative examples are shown in the polarized light micrographs of Fig. 2(a)–(d) for PEs crystallized at 110 °C. At this T_c the homopolymer (not shown) and PEs up to ~6 mol% of defects develop spherulites with positive overall birefringence. PE5.8 develops circular spherulites with resolved extinction quarters as well as irregular objects, and appears as a

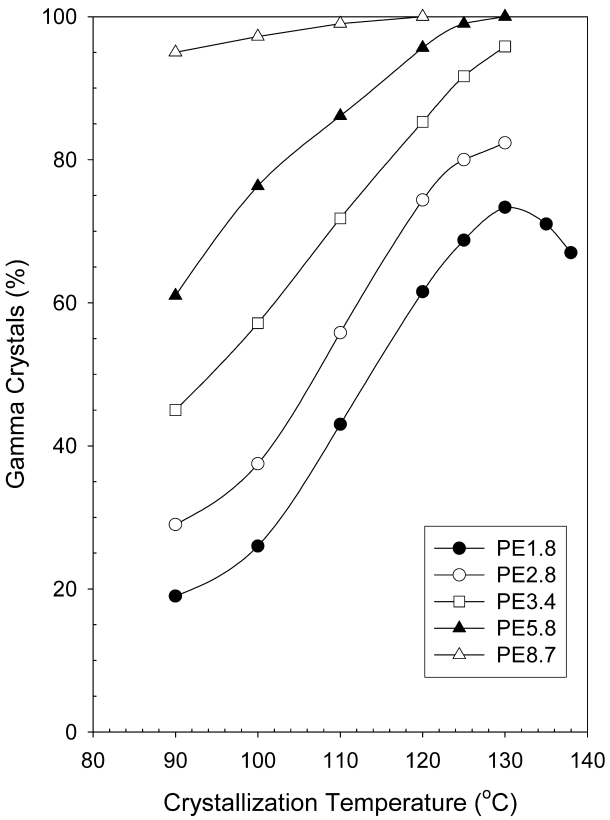

Fig. 2. Percentage of gamma phase as a function of crystallization temperature for propylene ethylene copolymers with ethylene content increasing from 0.8 to 7.5 mol%.

borderline copolymer for development of spherulitic structures. The copolymer with the highest ethylene content, PE8.7, forms small bundles of crystallites that organize in irregular, less birefringent dendritic structures. This copolymer shows an anomalous high nucleation density, which remained after recrystallization from a xylene solution, and is probably caused by a high concentration of residues from the catalyst [26].

The observed positive sign of the birefringence in all copolymers is reconciled with the schematic structural model of Fig. 1 and their fractional content of γ crystals. 'Parent' α lamellae that grow in the direction of the radial axis of the spherulite confer zero or negative sign to the birefringence while α or γ branching contribute with a positive sign. Furthermore, following the work of Binsbergen and DeLange [27], and assuming that all the orientations of the lamellae average over the complete volume of the spherulite, positively birefringent spherulites are expected when the fraction of lamellae tangentially grown from radially oriented ones is higher than one third. As seen in Fig. 2, at $T_c > 100$ °C all copolymers develop over 40% of the total crystallites in the gamma phase, most probably as epitaxial growth from α crystals. Therefore, in addition to orthogonal α lamellae branching from radial α-*i*PP, a high content of γ branching accounts for the observed positive birefringence. It was also found that both

polymorphs appear at about the same time in the early stages of the crystallization process [4]. Since there was no evidence of two types of spherulites, both α and γ lamellae must grow simultaneously within the same spherulite, likely following the α−γ branching structural relation as shown in Fig. 1 [23].

Increasing T_c to 125 °C the % of γ crystals increases from 60 to 100% in the PE series. However, the spherulitic pattern shows a similar behavior as shown in Fig. 4. Independent of the concentration of γ phase, the transition from spherulitic to non-spherulitic behavior occurs at a level of ~6 mol% total defects [28]. The copolymer with the highest concentration of ethylene, PE 8.7, develops 100% γ crystals as irregular objects that appear dendritic in nature and lack organized radial growth with weak mixed birefringence (Fig. 4(d)). A low concentration of crystallizable sequences and a possible compensation of crystals orientation contribute to the low birefringence.

Earlier works in low molar mass homopolymers or commercial *i*PPs crystallized under high pressure have shown spherulitic morphologies when the polymers crystallized in the pure gamma phase [24,29]. The micrographs of Figs. 3 and 4 evidence that PE copolymers may also crystallize almost completely in the gamma phase and still display a spherulitic morphology. Thus, it is the concentration of comonomer (or defects), not the development of γ phase, which disrupts the spherulitic lamellar arrangement. This is borne out by reference to the interiors of the quenched PE series, which show the same morphological variation and yet lack any significant amount of the γ phase [30].

In summary, the optical micrographs of Figs. 3 and 4 reveal the restriction placed by the presence of the comonomer (and other defects) on the maximum crystallizable sequence length and, hence, on the ability to propagate long radially oriented lamellae typical of alpha crystals. Absence of these long lamellae in highly defected iPPs preclude branching and a specific molecular orientation that in copolymers with lower ethylene contents leads to extinction quadrants and positively birefringent spherulites.

The intraspherulitic details of the type and orientation of lamellae for three PE copolymers crystallized at 110 °C are shown in the AFM phase images of Fig. 5. Both 5 × 5 and 2 × 2 μm images are given so as to distinguish lamellar orientation as well as details of lamellar branching. The homopolymer and the lowest defected copolymer, both with approximately 40% γ, display the most common morphology observed in *i*PP with low defect content, long radially oriented lamellae that emanate from a common center are seen with tilted and transverse branching in the intervening regions (Fig. 5(a) and (b)). Lamellae branching at ~90° and at ~40°, consistent with the structural characteristics of the α−α and α−γ branching can be identified in the 2 μm image. As comonomer content increases, paralleling a higher concentration of crystallites

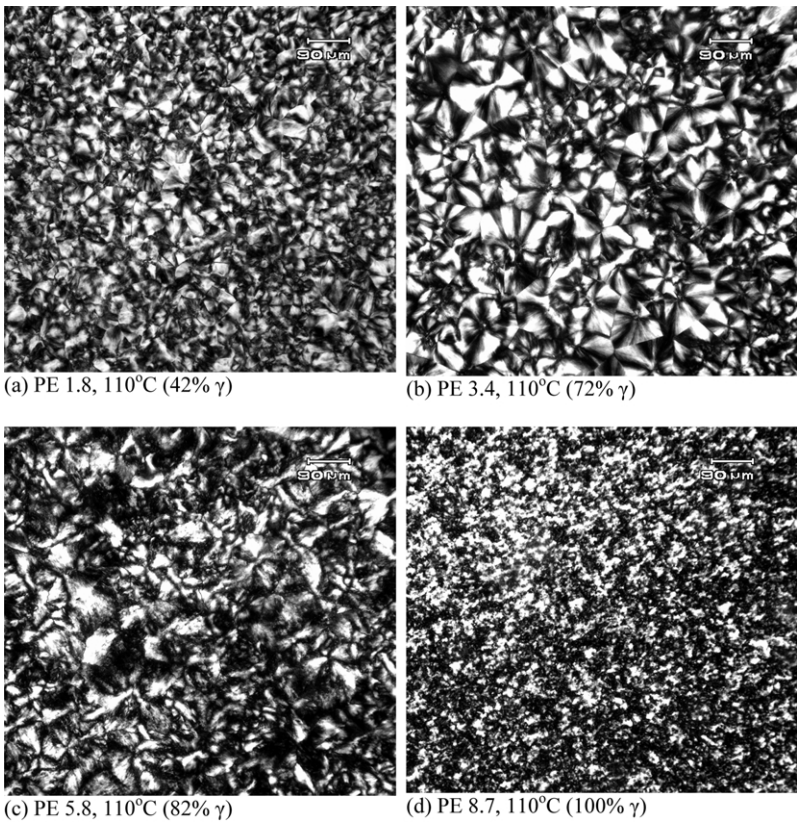

(a) PE 1.8, 110°C (42% γ) (b) PE 3.4, 110°C (72% γ)

(c) PE 5.8, 110°C (82% γ) (d) PE 8.7, 110°C (100% γ)

Fig. 3. Optical micrographs of propylene ethylene copolymers crystallized isothermally at 110 °C; (a) PE 1.8, (b) PE 3.4, (c) PE 5.8 and, (d) PE 8.7.

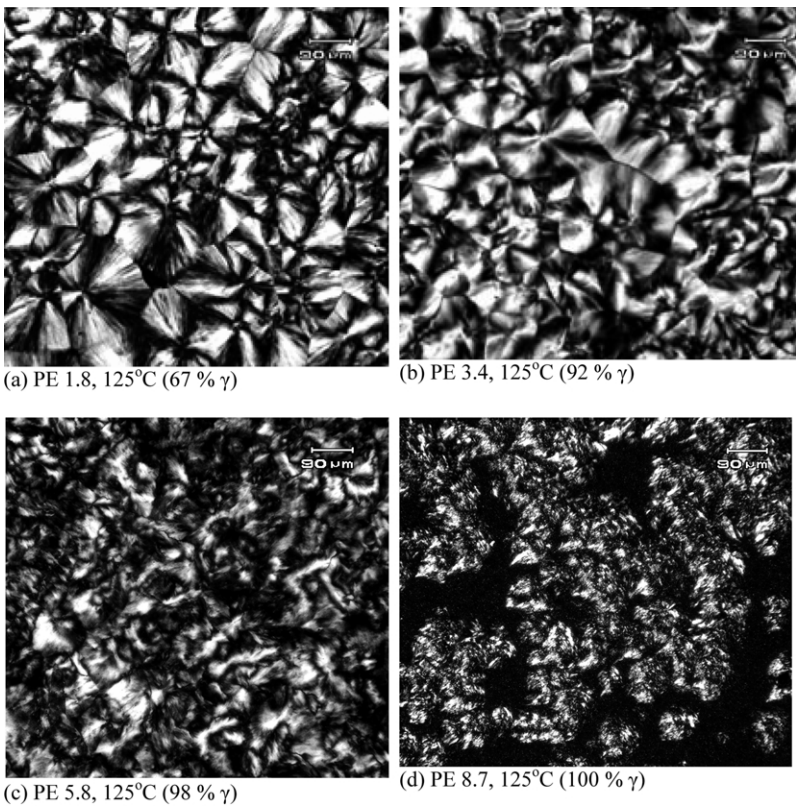

(a) PE 1.8, 125°C (67 % γ) (b) PE 3.4, 125°C (92 % γ)

(c) PE 5.8, 125°C (98 % γ) (d) PE 8.7, 125°C (100 % γ)

Fig. 4. Optical micrographs of propylene ethylene copolymers crystallized isothermally at 125 °C; (a) PE 1.8, (b) PE 3.4, (c) PE 5.8 and, (d) PE 8.7.

in the γ phase, radial lamellar growth is increasingly substituted by short lamellae that appear outgrowing tangentially to the structural growth axis (Fig. 5(c) and (d)). This is the expected appearance of γ-*i*PP branching from (presumable hidden) alpha lamellae in an ideal spherulite, built according to the structural model of Fig. 1, in which the parent α lamellae is seen edge on and oriented in the radial axis of the spherulite. At a level of 8.2 mol% defects, with 100% γ (Fig. 5(e) and (f)), the lamellae are significantly shorter and organized in bundles or stacks with no spherulitic pattern and no evidence of the radials. Cross hatching and other types of lamellar branching is diminished or not observed in these images, thus, reinforcing the notion that the mechanism that leads to branching from an α 'parent' lamellae results in normal growth for the γ [21].

Similar lamellar features were found in the interior of selected isothermally crystallized copolymers indicating that the observed surface AFM morphology is also characteristic for the bulk specimens. The change in lamellar texture with increasing % γ is striking. On this basis, one expects that departure of γ rich morphologies from the classical spherulites with radially oriented lamellae and branches diverging radially from them, will impact deformation and mechanisms of crystal growth, especially concerning direction of lamellar growth as it relates to spherulitic linear growth.

A gradual degradation of the extent and character of lamellae with increasing comonomer content was also observed in random ethylene-based copolymers [31,32]. However, these copolymers do not develop a crystallographic phase similar to the γ phase of *i*PP, with anti parallel chains favored by short crystallizable sequences. Consequently, in ethylene copolymers the character of the lamellae is lost at much lower defect contents ($\geq$4 mol%) [31,32]. Hence, it appears that the feasibility of formation of the gamma polymorph, with its tilted, near normal chains, plays a fundamental role in propagating lamellar crystallites in poly(propylene) and its copolymers up to a relatively high concentration of defects. The concentration and distribution of defects in the chain limits the long-range lamellar order.

Increasing crystallization temperature increases the fractional content of the gamma polymorph [4] and morphologies associated with transverse γ growth are found at lower concentrations of defects. This is seen in Fig. 6 for representative AFM images of PEs crystallized at 125 °C. PE 1.8 and PE 3.4 develop well formed spherulites and, respectively, 67 and 92% γ, and display a type and lamellar orientation very similar to that of samples PE 3.4 and PE 5.8 crystallized at 110 °C which developed similar levels of γ content (see Fig. 5(c)–(f)). Therefore, the morphologies parallel those found at lower T_c for the same content of γ crystals. Radially oriented (α) lamellae are hardly observed at these conditions for PEs with a content of defects $>\sim$3 mol%, in agreement with the nearly 100% γ developed. Yet, the AFM images suggest an orientation of γ lamellae consistent with the orientation expected for γ

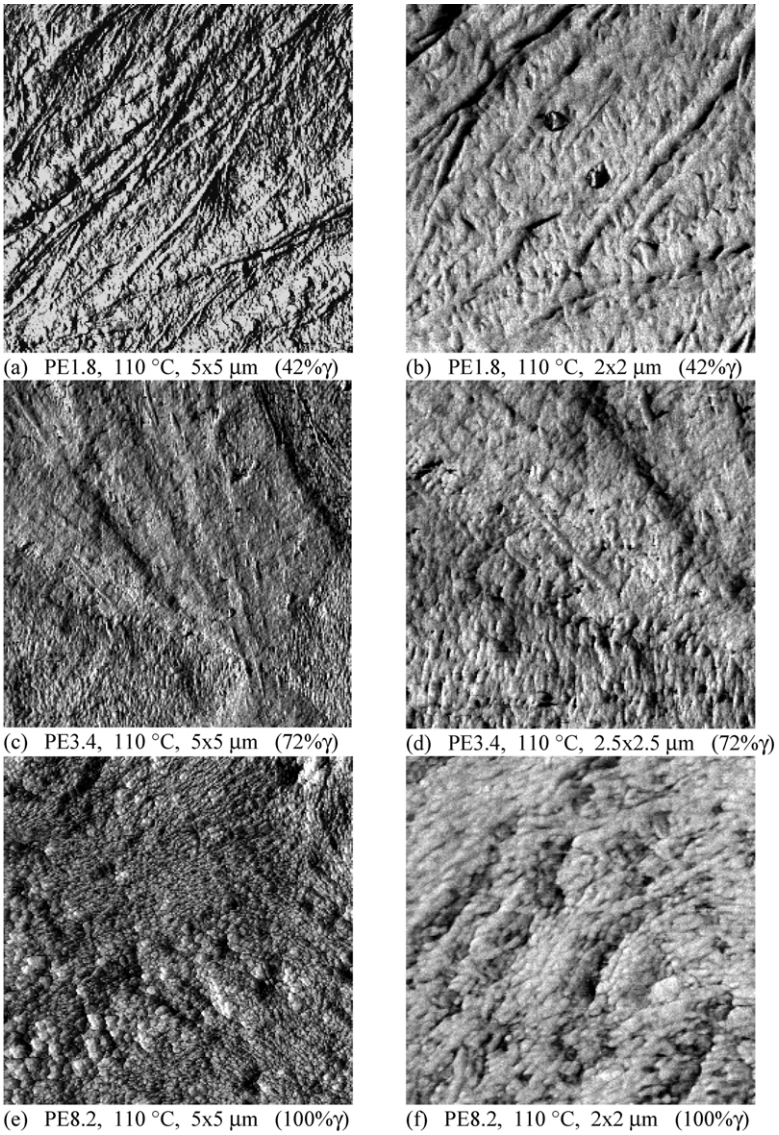

Fig. 5. AFM phase images of propylene ethylene copolymers crystallized at 110 °C; PE 1.8, (a) 5 × 5 μm (b) 2 × 2 μm. PE 3.4, (c) 5 × 5 μm (d) 2 × 2 μm. PE 8.2 (e) 5 × 5 μm (f) 2 × 2 μm. The content of gamma phase is indicated.

branching from α laths, i.e. appear transverse to the radial axis of the spherulite or bundle. As mentioned earlier, the specific origin of this orientation (found in both the surface and interior of the specimens) is unknown. It has been speculated that preexisting α seeds may direct the prevailing γ lamellar structure. On this issue optical micrographs of the structures that develop at the early crystallization stages seem to support the role of small contents of α phase in setting the lamellar orientation. One example is given in Fig. 7 for PE5.8 crystallized at 120 °C. The total 5% content of α phase is developed at the initial crystallization stages [4]. The objects shown in the micrograph originated as elongated structures with positive birefringence and, therefore, are consistent with α 'quadrites' that probably developed from the longest crystallizable sequences. Simultaneous and further growth proceeds preferentially in the γ phase, branching from both arms of the quadrite with equivalent orientations and conferring a strong positive birefringence. These structures suggest that the initial α quadrite is responsible for the apparent tangential orientation of subsequent lamellar growth.

The morphological change with increasing content of gamma crystals is summarized schematically in Fig. 8. Within the spherulitic regime, at relatively low concentrations of gamma phase (<40%), branching of both α-*i*PP and γ-*i*PP from α-*i*PP occurs readily leading to a population of dense isotropically oriented radial lamellae and thinner cross-hatched ones in the intervening spaces. Increasing the concentration of the gamma polymorph up to ~70%, still within the spherulitic range, the population of radially oriented lamellae clearly diminishes favoring the distinctive orientation of γ-*i*PP. This is shown in the images of Fig. 5(c) and (d) where numerous transverse on-growths of short lamellae are present, typical of the gamma phase as also observed in the homopolymer [15,22,24]. Copolymers

(a) PE1.8, 125 °C, 5x5μm (67 %γ)

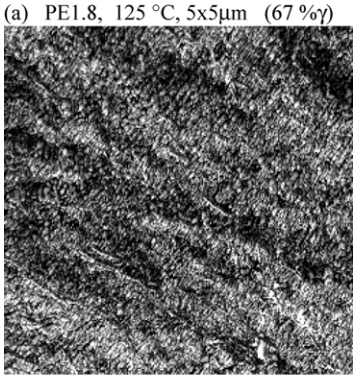

(b) PE3.4, 125 °C, 5x5μm (92 %γ)

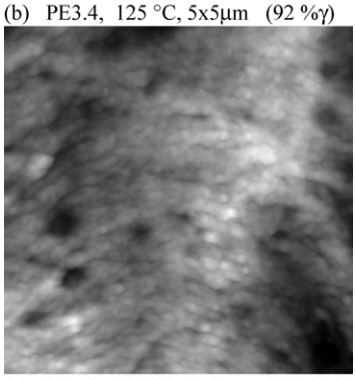

(c) PE5.8, 125 °C, 5x5μm (100 %γ)

Fig. 6. AFM images of propylene ethylene copolymers isothermally crystallized at 125 °C. (a) PE 1.8, (b) PE 3.4 and, (c) PE 5.8. The image size and content of gamma phase is indicated. Spherulitic radial axis in (a) and (b) is diagonal from top left to right bottom and it is vertical from bottom to top in (c).

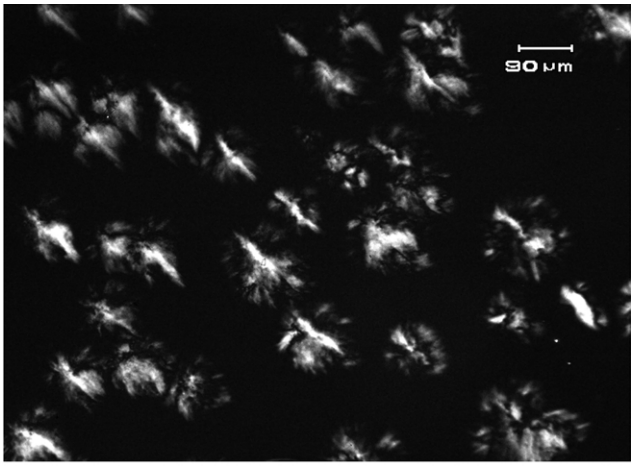

PE5.8, 120 °C (95 %γ)

Fig. 7. Optical micrograph of PE 5.8 (12 μm thin film) crystallized and observed at 120 °C. The elongated features with more intense birefringence probably developed from alpha 'quadrites'. See text for details on subsequent growth.

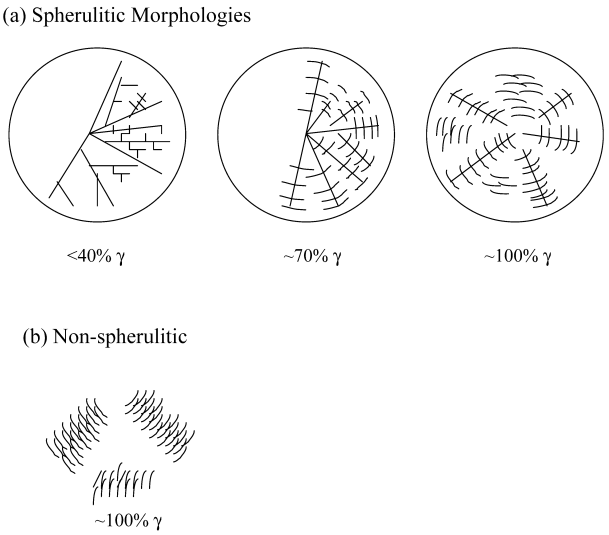

Fig. 8. Schematics models of edge-on lamellar textures with increasing crystalline gamma content for; (a) spherulitic structures and (b) unspherulitic, gamma rich textures.

that crystallize with >80% γ display quite remarkable morphologies. As seen in Figs. 5(e) and (f) and 6(b) and (c), radially grown lamellae are hardly observed. Instead, these copolymers display sporadic long stripes, possibly of hidden alpha laths [22], like spines, with profuse transverse lamellae emanating from them, as indicated in the schematics of Fig. 8. The volume between spines is covered with stacks of short lamellae that also appear transverse to the main structural growth, consistent with a predominantly unidirectional orientation of γ-*i*PP. A similar morphology was observed in a homo poly(propylene) that also developed a very high concentration of gamma phase (>85%) [24]. The relevance of the present results is that they make evident the continuous change in intraspherulitic orientation and lateral dimension of the lamellae with increasing concentration of the γ phase. In addition, a systematic change in crystalline texture with increasing comonomer content and crystallization temperature is documented for these copolymers.

Propylene 1-hexene copolymers display similar morphological changes on increasing defect content as the propylene ethylene series discussed above. However, the non-crystallizability of the l-hexene comonomer and, thus, the reduced crystallizable sequence length compared to the propylene ethylene series shifts the γ content in the PH series to higher values [4].[1] The morphologies associated with high contents of γ are, thus, observed at lower

[1] Since the equilibrium melting temperatures of these copolymers are unknown, a proper comparison of properties at the same undercooling is not presently feasible.

1-hexene contents. In addition, the overall defect content at which the spherulitic pattern is lost shifts to significantly lower values, ~3 mol%, compared to ~6 mol% in PEs. These features are illustrated in the two representative AFM images of Fig. 9 for PH 2.2 (65% γ) and PH 3.5 (90% γ) crystallized at 120 °C. PH2.0 forms spherulites with radial lamellae and profuse short transverse branching consistent with both α and γ branching. In the non-spherulitic PH 3.5, short lamellae are grouped in bundles displaying the homogeneous orientation transverse to the structural growth, typical of the high concentrations of γ lamella in this polymer. Comparatively this type of morphology was observed for a PE copolymer with significantly higher ethylene content (PE 8.2, Fig. 5(e)).

3.3. Effect of comonomer type on lamellar morphology

In this section, the spherulitic and lamellar morphology of copolymers with very similar contents of ethylene, 1-butene, 1-hexene or 1-octene comonomer (~3.3 mol %) are compared.

Significant differences in polymorphic and melting behaviors were previously observed between these four copolymer types when the data are compared for the same total defect concentration and same crystallization temperature [4]. PH and PO crystallize at any temperature at slower rates and develop higher concentrations of the gamma polymorph than any of the other two copolymers. This experimental observation confirmed the NMR findings that the ethylene and l-butene units are included in the crystalline lattice [3,33,34]. The interest here is to investigate how a different partitioning of the comonomer unit between crystalline and non-crystalline regions affects the overall spherulitic and intraspherulitic lamellar morphology. As representative examples, the series of SEM and AFM images of the four copolymers with ~3.3 mol% defects crystallized at 125 °C are given in Fig. 10. The SEM and AFM images of PB3.4 show coarse spherulites with a relatively large population of radially oriented lamellae. PE3.4 with a higher γ content, displays a higher population of related transverse branching. In contrast, the organization of the irregular bundle-type morphologies of PH 3.4 and PO2.9 is only resolved in the SEM images. Following the schematics presented in Fig. 8, short gamma crystals within each bundle preserve a transverse orientation. At any crystallization temperature the morphologies of these two types of copolymers are very similar, paralleling their similarity in crystallization behavior and the development of the same concentration of the gamma phase [4], resulting from the same crystallizable sequence lengths.

The images of this series (Fig. 10) reflect the difference in co-crystallizability of the co-unit at the spherulitic and lamellar scales. At the micrometer level the shorter crystallizable sequences of PH 3.5 and PO 2.9 hinder crystallinity and lateral extension of the lamellae. Therefore, the spherulitic pattern is perturbed, while at the nano-

Fig. 9. AFM phase images of propylene 1-hexene copolymers isothermally crystallized at 120 °C; (a) PH 2.2 and, (b) PH 3.5. The image size and content of gamma phase is indicated.

structural level a greater ability to form the γ polymorph of copolymers with co-units rejected from the lattice, diminishes or eliminates radial lamellae.

3.4. Lamellar thickness distributions from AFM images

Long periods of at least 80 different lamellae from each specimen were measured from flat and edge on lamellae following the technique detailed in the experimental part. Representative examples of these measurements are given in Fig. 11(a) and (b).

Width measurements were recorded from valley to valley in the topographic profiles and, for parallel arrays of edge on lamellae, correlate with the lamellar long period (Fig. 11(a)). Symmetric height profiles from flat surfaces were also systematically recorded and taken as long periods (Fig. 11(b)). This assessment was based on the results of Sutton et al. [7] that etching times between 5 and 30 min do not affect the value of the step heights. It was also assumed that for these copolymers the permanganic etchant efficiently removed the non-crystalline layer from the surface leaving the layer underneath the crystal intact. We are aware of the large uncertainties involved in these measurements and the difficulty in identifying the exact lamellae orientation when both α and γ phases coexist as in most of the copolymers analyzed. For example, in an ideal configuration such as that of Fig. 1 with radially oriented α parent lamellae, and γ branching, the thickness and

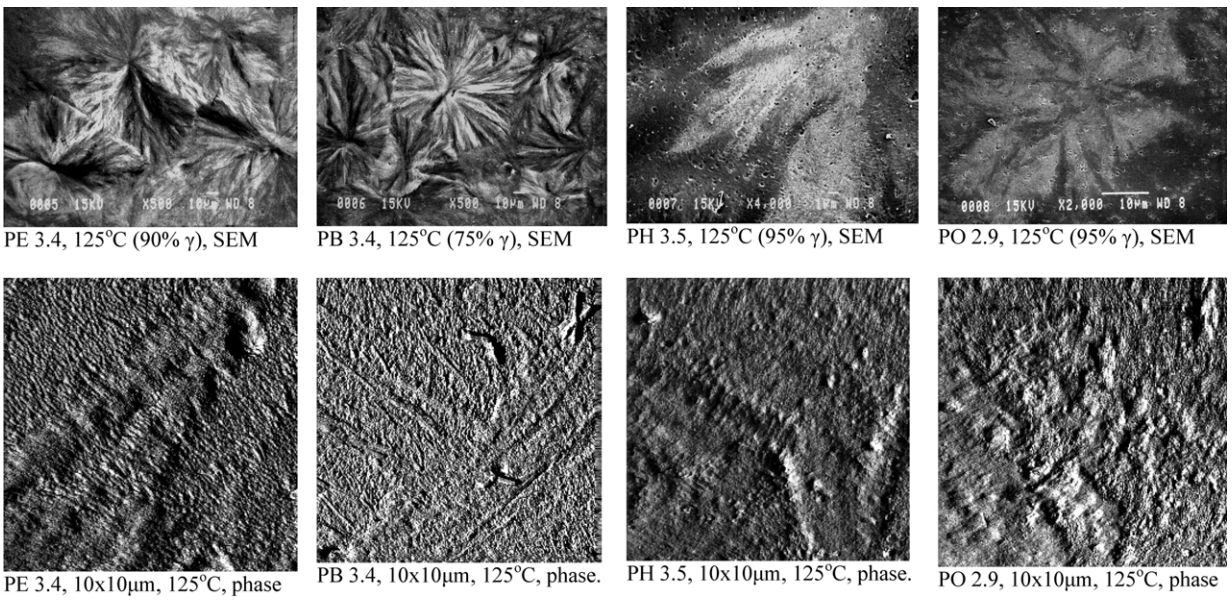

Fig. 10. SEM and AFM micrographs of different types of copolymers with 3.3 mol% defects crystallized at 125 °C. Top row (from left to right), SEM images of PE 3.4, PB 3.4, PH 3.5 and PO 2.9. Lower row (from left to right), AFM phase images of PE 3.4, PB 3.4, PH 3.5 and PO 2.9. The image size and content of gamma phase is indicated.

periodicity between α lamellae is the same when observed edge-on from any angle. The thickness and periodicity of γ lamellae that grow at 40° from the radial axis is, however, different by 1.55 (1/sin40°) when viewed edge-on from the ab plane or at a right angle to this direction (the bc plane of the γ phase). Hence, a careful selection of lamellae with clear orientations is needed, such as is occasionally obtained from very thin films or from dilute solution, to ascertain possible differences between the stem lengths of α and γ lamellae that may correlate with their melting behavior [4,35]. In this work when γ lamellae appeared oriented with their ab face edge on, as for example in Fig. 11(a) and most of Fig. 5(d), the measured periodicity was multiplied by sin 40°. This correction assumes a uniform tilted orientation

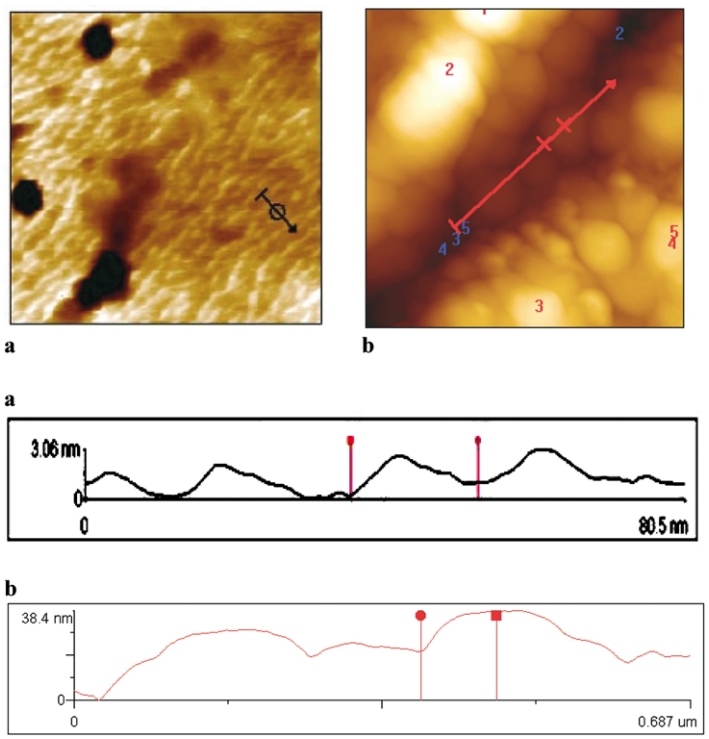

Fig. 11. Representative examples of section profiles for measurements of lamellar long periods. (a) Edge on lamella in PE 5.8 crystallized at 120 °C, (b) topographic image of flat on lamellae in PE 2.2 crystallized at 130 °C. Profiles correspond to sections along the indicated lines in the respective micrograph.

within these crystals, as in the schematics of Fig. 1. In this way the measured data can be compared with the SAXS long periods obtained in the same samples. Rather than reporting isolated absolute values, we analyze patterns of the thickness distributions in the copolymer series. Results that are systematic and are also in agreement with other techniques will raise the degree of confidence in the AFM measurements.

Representative histograms of the distribution of long periods for the series of propylene ethylenes crystallized at 110 °C are given in Fig. 12(a). In general the distributions appear broad and asymmetric for all copolymers.[2] The homopolymer and PE 1.8, both with similar defect content, display almost identical unimodal periodicity distribution centered at about 17 nm. The distributions broaden considerably and appear bimodal for PE2.8 and in copolymers with 50 ± 10 mol% γ.

Increasing concentration of defects and, paralleling the increase in γ content, the distribution becomes narrower and the mean value shifts to considerably lower values. The change in width conforms to a more uniform lamellar orientation as observed in the AFM images, and the shift to lower values to a reduction in length of crystallizable sequences with increasing defects. The limitations in the minimum measurable thicknesses associated with the tip radius also add a boundary to the lower end of the distribution. It is expected that, with increasing defects, the thickness of the crystallites will be restricted and a larger intercrystalline region will develop. To propagate the lateral extension of the lamellae, crystalline sequences from different molecules will need to be transported to the growing site. This transport process, although less restricted in forming γ-*i*PP crystallites than in other copolymers in which a crystalline cell with tilted molecules is not feasible [4,35], is hindered by entanglements in the viscous melt, and contributes to the relatively broad interlamellar regions. Broad, thick interlamellar regions have been previously shown to be typical of copolymers [32].

The distributions of long periods measured in the PH series display similar trends but are centered at ~3 nm lower values compared to the PE series. This difference is also maintained when the long spacing data are corrected by the crystallinity obtained by WAXS and explains the lower melting of these copolymers compared to matched propylene ethylenes [4,36]. Hence, the measurements of periodicities in real space from AFM images follow the expected systematic trends, which are qualitatively in line with the observed morphologies and the DSC melting behavior [4,29,36]. This result gives us confidence in using such distributions to obtain the average lamellar long periods in these copolymers to be compared with SAXS data. The distributions of copolymers with ~3.3 mol% defects crystallized at 125 °C are given in Fig. 12(b). In line with morphological data, the PB copolymer with the lowest concentration of γ phase (75%) displays the broadest distribution and the highest mean value, PH and PO copolymers develop ~95% γ and display noticeably thinner lamellar periodicities.

Mean values of the long period and standard deviations are plotted as a function of defect content in Fig. 13 for copolymers crystallized at 110 °C. AFM data are shown as filled symbols and the open symbols are long periods obtained from SAXS. The lines in this figure are linear regressions over the AFM data for the PE series (solid) and PH series (dashed). Under any given crystallization condition, within each series, the long period decreases with increasing defect content by ~10 nm within the range studied. Two main trends are clearly shown; the data for PEs and the PB studied are significantly higher than those of PHs and PO and the greatest divergence of periodicities between the series is found at the highest comonomer contents. The mean long period of copolymers with ~3.3 mol% defects crystallized at 110 °C decreases from 18 to 15 nm and to ~10 nm for PB, PE and PH, respectively. Therefore, lamellar periodicity also reflects the less severe restriction on the availability of crystallizable sequences in both PB and PE copolymers. In spite of the large uncertainty associated with these measurements, the AFM determined long period of any copolymer was found to shift to higher values with increasing crystallization temperature and to maintain similar systematic trends with comonomer content as for crystallization at 110 °C.

When the long periods are corrected with the crystallinity fraction derived by WAXS the trends seen in Fig. 13 are maintained, suggesting that crystallite thickness decreases with increasing defect content within the series. A decrease in α and γ lamellar thickness is consistent with the observation that the melting temperature also decreases with comonomer or total defect content [4,36]. Insofar as Flory's equilibrium theory [37] can be taken as a reference point for the PH and PO copolymer series in which the comonomer is clearly rejected from the lattice [34], the decrease in crystallite size with increasing comonomer content adheres to thermodynamic expectations. The present results are at variance with those of Strobl et al. [38] who found no effect of comonomer content on the crystallite thickness measured by SAXS in syndiotactic propylene 1-octene copolymers. Our AFM results do not support the multi-step process of formation and growth of lamellae crystallites derived upon the thickness invariance and from the granular appearance of microscopy images of polymeric lamellae [39,40].

Interestingly, independently of the fraction of γ crystallites developed, all copolymers show broad single SAXS peaks and periodicities with small or negligible changes with increasing defect content or among the various types of copolymers. The greater differences between SAXS and AFM data are found in the range of lower defect content. This is attributed to the difficulty of interpreting the origin of

[2] Mismatch in lamellar orientations may contribute to the breath of the distributions.

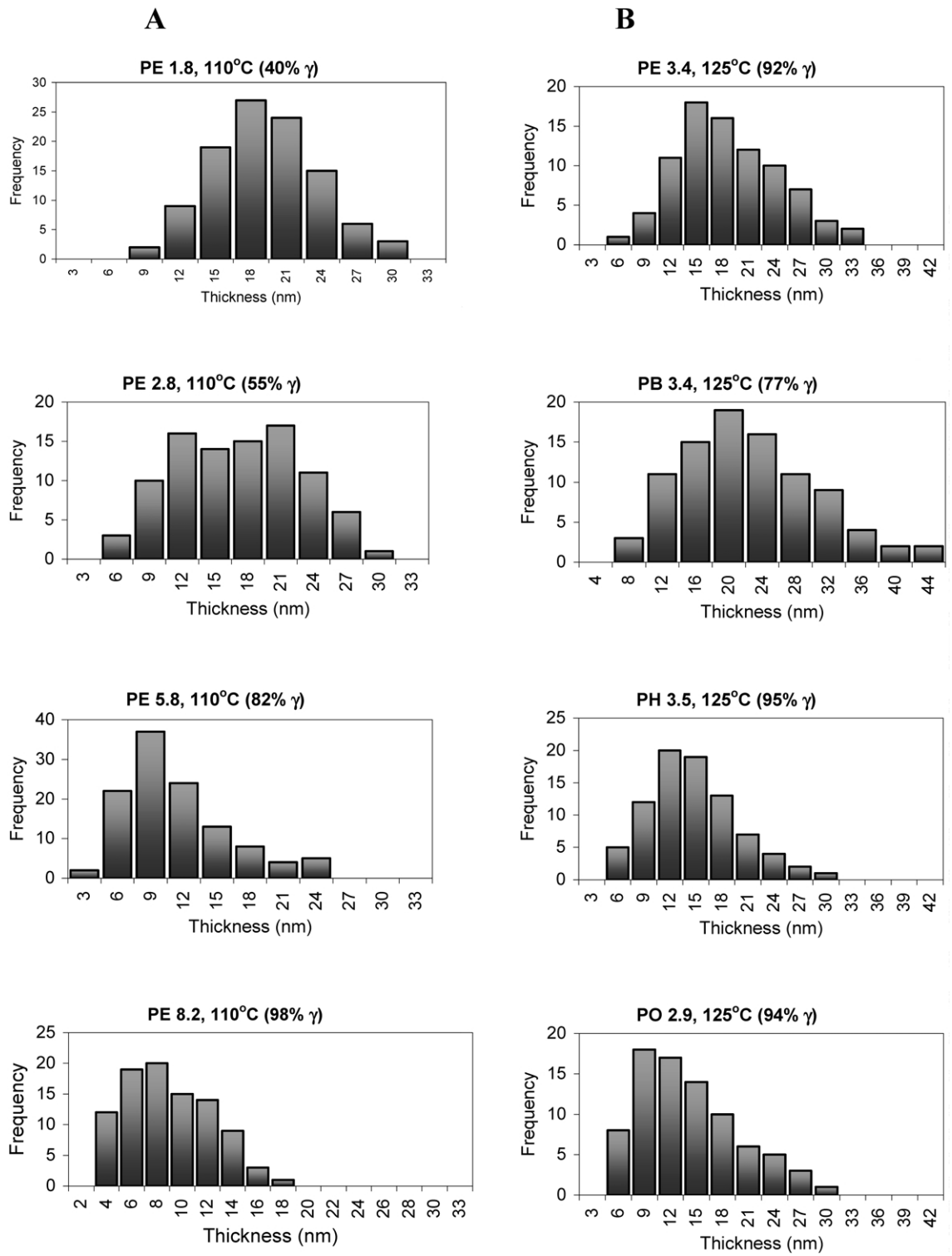

Fig. 12. Representative histograms of lamellae long spacings showing distributions obtained from AFM measurements for (a) series of PE copolymers with increasing ethylene content crystallized at 110 °C and, (b) different types of propylene copolymers with ~3.3 mol% total defects crystallized at 125 °C. The copolymer type and content of gamma phase is indicated.

the diffuse SAXS maximum when complex lamellae morphologies, lacking ordered stacks, develop. A typical example is the topographic image of Fig. 14(a) obtained for PB 3.4 crystallized at 110 °C (65% γ). Scattering over this type of lamellar structure leads to a broad single peak (Fig. 14(b)) that averages all crystal orientations, including the smallest, and may not reflect two periodicities associated with the apparent dual type of lamellae. Analysis using the

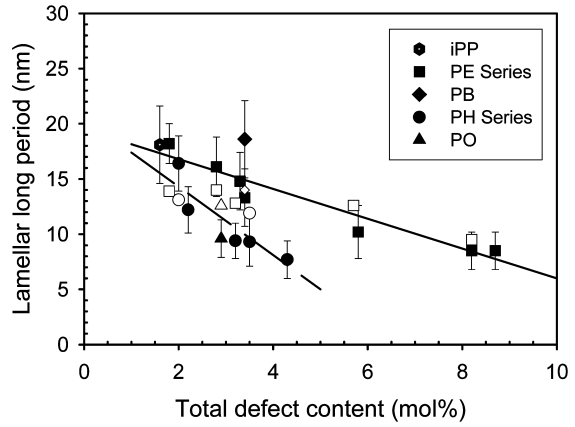

Fig. 13. Mean values and standard deviations of lamellar long period measured by AFM (closed symbols) and SAXS (open symbols) for propylene copolymers isothermally crystallized at 110 °C. Solid line: linear regression over AFM data of propylene ethylenes. Dashed line: linear regression over AFM data of propylene 1-hexenes and propylene 1-octene.

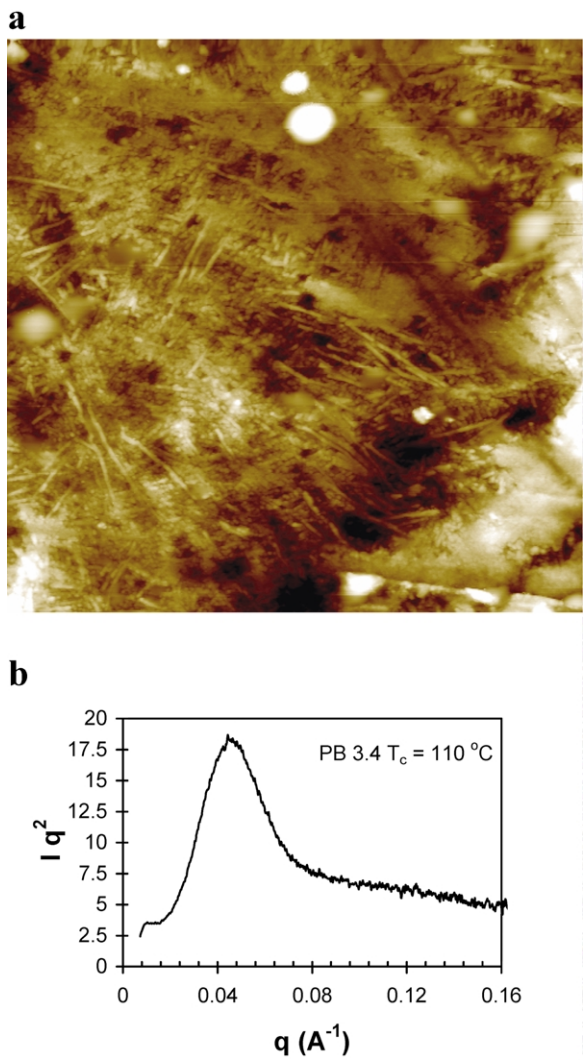

Fig. 14. (a) Topographic AFM 5 × 5 μm image of PB 3.4 crystallized at 110 °C (64% γ phase). (b) Lorentz corrected SAXS data of same copolymer.

interface distribution function did not yield the expected bimodal population of thicknesses either, as also found in the analysis of a homopolymer [41,42]. AFM, on the other hand, measures the long spacing of individual lamellae but may not resolve the smaller population of crystallites. Agreement between both techniques for these non-stacked lamellar morphologies is not expected. Conversely, γ rich morphologies display a long-range periodicity of lamellar stacks, and a better agreement between the values of AFM and SAXS is expected. The SAXS data in Fig. 13 closely follow these expectations. Good agreement between AFM and SAXS was found in quantitative analysis of a different system with lamellae stacks [43]. These extensive data confirm that a careful analysis of the AFM images can lead to quantitative periodicity thicknesses in real space in addition to identifying lamellar profiles and orientation.

4. Conclusions

AFM studies, guided by previous thermodynamic and crystallographic investigations [4,12,23] have revealed some striking morphological features of the crystalline state of these copolymers. At the supermolecular level a clear distinction in morphologies appears between copolymers with co-units that partially co-crystallize with the propylene unit (PE and PB), and copolymers with l-hexene and l-octene units that are rejected from the propylene crystalline lattice. While spherulites are formed in copolymers with up to ~6 mol% defects in the first group, the spherulitic habit is lost at ~3 mol% defects in the second. The development of the γ polymorph, as the defect content or crystallization temperature increases, has a marked effect on the lateral extent and orientation of lamellae either in spherulitic or bundle-like (dendritic) structures. Schematics of this behavior are provided in Fig. 8. As the fraction of γ crystallites increases from 40 to ≥70% radially oriented lamellae and intervening cross hatching associated with α-*i*PP, are substituted for heavily tilted γ branching. Due to the equivalence in orientation of γ-*i*PP branching from parent or daughter α-*i*PP, γ rich morphologies appear as a dense array of short lamellae transverse to the macroscopic growth. Remarkably, lamellae are observed in copolymers with a significantly high concentration of defects (up to ~9 mol%), lending relevance to the role of the gamma phase in propagating lamellar-like crystallites in highly defective poly(propylenes).

Increasing structural irregularities in the copolymer chain affects lamellar long periods in a manner that follows the decrease of melting points measured by DSC [4,34]. In addition, at any given comonomer content, PH and PO copolymers have lower lamellar periodicities than those of ethylene or 1-butene based copolymers in line with the reduced average crystallizable sequence length in the former pair [4]. The long periods measured by SAXS only agreed with AFM data for γ rich copolymers for which a

relatively uniform stacked lamellar morphology develops. Limitations of the SAXS technique for samples containing complex lamellar morphologies were discussed. The AFM technique was found to be a reliable marker in measuring in real space lamellar periodicities. It also seems a sensitive one, particularly where the morphology does not involve clear lamellar stacking and, thus, is not amenable to meaningful quantification by SAXS.

Acknowledgements

Funding of this work by the National Science Foundation, grant numbers DMR-0094485 and DMR0076485 (instrumentation grant) is gratefully acknowledged. We acknowledge the help of Kimberly A. Riddle with SEM imaging and are also grateful to S. Magonov for his assistance with AFM in the initial stages of this project. Helpful comments from one reviewer about orientation and thicknesses of epitaxial γ lamellae are also acknowledged. The research at Oak Ridge was sponsored in part by the U.S. Department of Energy under Contract No. DE-AC05-000R22725 with the Oak Ridge National Laboratory, managed by the UT-Battelle, LLC.

References

[1] Brintzinger HH, Fischer D, Mülhaupt R, Rieger B, Waymouth RM. Angew Chem, Int Ed 1995;34:1143.
[2] Busico V, Cipullo R. Prog Polym Sci 2001;26:443.
[3] Alamo RG, Vanderhart DL, Nyden MR, Mandelkern L. Macromolecules 2000;33:6094.
[4] Hosier IL, Alamo RG, Esteso P, Isasi JR, Mandelkern L. Macromolecules 2003;36:5623.
[5] Olley RH, Hodge AM, Bassett DC. J Polym Sci, Polym Phys Ed 1979; 17:627.
[6] Schönherr H, Snétivy D, Vancso GJ. Polym Bull 1993;30:567.
[7] Sutton SJ, Izumi K, Mijaji H, Fukao K, Miyamoto Y. Polymer 1996; 37:5529.
[8] Zhou H, Wilkes GL. Polymer 1997;38:5735.
[9] Trifonova D, Varga J, Vancso GJ. Polym Bull 1998;41:341.
[10] Trifonova-Van Haeringen O, Varga J, Ehrenstein GW, Vancso GJ. J Polym Sci, Part B: Polym Phys 2000;38:672.
[11] Vancso GJ, Beekmans LGM, Pearce R, Trifonova D, Varga J. J Macromol Sci, Phys 1999;B38:491.
[12] Brückner S, Meille SU, Petraccone U, Pirozzi B. Prog Polym Sci 1991;16:361.
[13] Lotz B, Wittman JC, Lovinger AJ. Polymer 1996;37:4979.
[14] Khoury F. J Res Nat Bur St 1966;70A:29.
[15] Lovinger J. J Polym Sci, B: Polym Phys 1983;21:97.
[16] Lotz B, Wittman JC. J Polym Sci, Polym Phys Ed 1986;24:1541.
[17] Geil PH. Polymer single crystals. New York: Interscience; 1963. p. 214.
[18] Padden Jr FJ, Keith HD. J Appl Phys 1966;37:4013.
[19] Lotz B. J Macrom Sci Part B 2002;B41:685.
[20] Chi C. MS Thesis, Florida State University; 1997.
[21] Meille SU, Brückner S, Porzio W. Macromolecules 1990;23:4114.
[22] Lotz B, Graff S, Wittman JC. J Polym Sci, B: Polym Phys 1986;24: 2017.
[23] Lotz B, Graff S, Straupe S, Wittman JC. Polymer 1991;32:2902.
[24] Thomann R, Wang C, Kressler J, Mülhaupt R. Macromolecules 1996; 29:8425.
[25] Meille SU, Ferro DR, Brückner S. Macrom Symp 1995;89:499.
[26] Alamo RG, Blanco JA, Agarwal PK, Randall JC. Macromolecules 2003;36:1559.
[27] Binsbergen FL, De Lange BG. Polymer 1968;9:23.
[28] At very high crystallization temperatures (>130 °C), low kinetics coupled with depletion of crystallizable sequences lead to open spherulites or more disordered structures.
[29] Mezghani K, Phillips PJ. Polymer 1997;38:5725.
[30] Alamo RG, Hosier IL. To be published.
[31] Chen HY, Chum SP, Hiltner A, Baer E. J Polym Sci, B: Polym Phys 2001;39:1578.
[32] Voigt-Martin IG, Alamo RG, Mandelkern L. J Polym Sci, B: Polym Phys 1986;24:1283.
[33] Nyden MR, Vanderhart DL, Alamo RG. Comp Theor Comp Sci 2001; 11:175.
[34] Alamo RG, Isasi JR, Kim M-H, Mandelkern L, VanderHart DL. Polym Mater Sci Eng Proc 1999;81:346.
[35] Alamo RG, Kim M-H, Galante MJ, Isasi JR, Mandelkern L. Macromolecules 1999;32:4050.
[36] Hosoda S, Hori H, Yada K, Nakahara S, Tsuji M. Polymer 2002;43: 7451.
[37] Flory PJ. Trans Faraday Soc 1955;51:848.
[38] Hauser G, Schmidtke J, Strobl G. Macromolecules 1998;31:6250.
[39] Strobl G. Eur Phys J 2000;E-3:165.
[40] Heck B, Hugel T, Iijima M, Sadiku E, Strobl G. New J Phys 1999;17: 1.
[41] We thank Mr T-Y. Cho, Prof D.Y. Yoon for performing the interface distribution calculation.
[42] Campbell RA, Phillips PJ, Lin JS. Polymer 1993;34:4809.
[43] Basire C, Ivanov D. Phys Rev Let 2000;85:5587.